
Article:
Shen, Lu, Henson, Benjamin, Zakharov, Yury orcid.org/0000-0002-2193-4334 et al. (1 more author) (2020) Adaptive Nonlinear Equalizer for Full-Duplex Underwater Acoustic Systems. IEEE Access. pp. 108169-108178. ISSN 2169-3536

https://doi.org/10.1109/ACCESS.2020.3000590

IEEE Access
Multidisciplinary | Rapid Review | Open Access Journal

Received May 1, 2020, accepted June 1, 2020, date of publication June 8, 2020, date of current version June 22, 2020.

Digital Object Identifier 10.1109/ACCESS.2020.3000590

Adaptive Nonlinear Equalizer for Full-Duplex Underwater Acoustic Systems

LU SHEN, (Graduate Student Member, IEEE), BENJAMIN HENSON, (Member, IEEE), YURIY ZAKHAROV, (Senior Member, IEEE), AND PAUL D. MITCHELL, (Senior Member, IEEE)

Department of Electronic Engineering, University of York, York YO10 5DD, U.K.

Corresponding author: Lu Shen (ls1215@york.ac.uk)

The work of Benjamin Henson, Yuriy Zakharov, and Paul D. Mitchell was supported in part by the U.K. Engineering and Physical Sciences Research Council under Grant EP/P017975/1 and Grant EP/R003297/1.

ABSTRACT To enable full-duplex (FD) operation in underwater acoustic systems, the strong self-interference (SI) from the near-end transmitter should be efficiently cancelled. Digital cancellation is considered as the main approach for the SI cancellation. It is believed that the key challenge in achieving a high level of cancellation is to overcome the nonlinear distortion in the transmit and receive chains. The majority of the nonlinearity is introduced by the power amplifier (PA), which can be dealt with by using the PA output as the reference signal for digital cancellation. Further nonlinearity comes mainly from the hydrophone pre-amplifier. For applications working in half-duplex mode, the pre-amplifier can normally be assumed to be linear due to the low received signal level. For FD operations, the strong SI might result in a nonlinear response of the pre-amplifier, and this nonlinearity should be equalized to achieve a high cancellation performance. In this paper, we propose a technique for equalizing the nonlinearity in the pre-amplifier. This is done using a basis expansion model of the nonlinear equalizer response. More specifically, the Legendre polynomials are used as the basis functions. The expansion coefficients are updated to reduce the mean squared error or a cost function derived based on the power spectrum of the received signal. The performance of the equalizer is evaluated using the experimental data with artificial nonlinear distortion and with real nonlinearity introduced by the hydrophone pre-amplifier. Both sets of results demonstrate that nonlinear distortions can be effectively equalized using the proposed adaptive equalization technique.

INDEX TERMS Adaptive equalization, BEM, full-duplex, nonlinear distortion, underwater acoustic communications.

I. INTRODUCTION

In-band full-duplex (FD) operation has demonstrated its ability to improve the channel capacity in terrestrial radio communications [1]–[3]. To make FD operation feasible, self-interference (SI) cancellation techniques have been proposed to achieve effective SI cancellation under typical hardware impairments such as the low-resolution analogue-to-digital converters (ADC) and power amplifier (PA) nonlinearity [4]. Existing techniques for FD in terrestrial radio communications cannot be directly applied for FD underwater acoustic (UWA) communications, since the limiting factors for SI cancellation are different due to the distinct environments. In UWA systems, high resolution ADCs can be used due to the relatively low frequencies of acoustic signals. Therefore, the front-end processing of the receiver can be done in the digital domain, thus avoiding hardware impairments such as the carrier frequency offset, in-phase and quadrature imbalance [5]. Most hydrophones have an integrated pre-amplifier to improve the signal to noise ratio (SNR) at the output. Pre-amplifiers have an almost linear response within a voltage limit. Beyond the limit, they become non-linear and saturate [6]. For FD UWA systems, the main limitation of SI cancellation is the nonlinearity introduced by the PA in the transmit chain [7], hydrophone pre-amplifier and transducers [8].

In the literature addressing nonlinear distortion in FD operations, most effort is spent on dealing with the nonlinearity introduced by the PA, either by using a nonlinear canceller based on the Hammerstein model to estimate the combined channel including the PA and SI channel [7], [9] or by pre-distorting the reference signal for digital cancellation based

The associate editor coordinating the review of this manuscript and approving it for publication was Emrecan Demirors.

on the estimate of PA characteristics [10], [11]. In [12], it is shown that the PA nonlinearity can be dealt with by using the PA output as the reference signal for digital cancellation. Without the limitation of PA nonlinearity, the major obstacle comes from the nonlinear distortion introduced by the hydrophone pre-amplifier. In most UWA applications, the received signal is expected to be relatively weak, such that the pre-amplifier operates in the linear mode. For FD operations, the received signal could be quite strong as it includes both the far-end signal and the strong near-end SI. To achieve a high level of SI cancellation, the nonlinear distortion introduced by the pre-amplifier must be taken into account.

In this paper, we propose an adaptive technique to equalize the nonlinear distortion introduced by the pre-amplifier. The equalization is done in the passband instead of baseband to avoid additional distortions due to the passband to baseband conversion. The equalization is done using a basis expansion model (BEM) which models the inverse of the pre-amplifier response. Here, the Legendre polynomials [13] are used as the basis functions. The BEM expansion coefficients are updated using a coordinate descent search to reduce the cost function. We consider two cost functions, the mean squared error (MSE) and a cost function derived based on the power spectrum of the received signal. Good equalization performance is guaranteed with the MSE-based cost function, but the complexity of this approach is high. Thus, we propose a spectrum-based cost function and show how the complexity can be further reduced by recursive computations.

The performance of the proposed equalizer is evaluated through two sets of water tank experiments. For the first set of experiments, we use the received signal from a hydrophone without pre-amplifier and introduce an artificial nonlinearity based on the Rapp Model [14]. We show that the adaptive equalizer is capable of equalizing this nonlinearity. For the second set of experiments, the received signal from a hydrophone with pre-amplifier is used and the SI cancellation performance before and after nonlinear equalization are computed. The results show that up to 4 dB improvement can be achieved with the proposed equalizer. The contributions of this paper are summarized as follows:

- An adaptive equalization technique based on Legendre polynomials is proposed to equalize the nonlinear distortion introduced by a hydrophone pre-amplifier.
- The expansion coefficients of the basis functions are updated in a dichotomous way to reduce the cost function. Both the mean squared error (MSE) and a function derived based on the power spectrum of the received signal are used as the cost function. The latter approach significantly reduces the computational complexity.
- The performance of the adaptive equalizer is evaluated through tank experiments, and it is shown that the nonlinear distortion introduced by the hydrophone pre-amplifier can be effectively equalized.

The rest of the paper is organized as follows: In Section II, the adaptive equalization technique is described in detail. In Section III, the performance of the equalizer is evaluated through two sets of water tank experiments. In Section IV, the conclusions are drawn.

II. SYSTEM MODEL

In this section, detailed descriptions of the FD UWA system and the adaptive nonlinear equalizer is given.

The block diagram of the FD UWA system with adaptive nonlinear equalization is shown in Fig. 1. At the transmitter, a sequence of complex modulated symbols $a(i)$ is pulse-shaped and up-shifted to the passband. The passband samples $s(n)$ are digital-to-analogue converted, amplified and emitted by a projector. After propagating through the SI channel, the SI channel output $r(t)$ along with the far-end signal $z(t)$ and noise $n(t)$ are received by the hydrophone.

Adaptive filters are generally used for SI channel estimation in FD UWA systems [15]–[17]. Here we use the recursive least square (RLS) adaptive filter for channel estimation due to its fast convergence speed. As shown in Fig. 1, the PA output is used as the regressor of the adaptive filters for SI cancellation. In such a case, the SI channel estimation performance can be significantly improved since the nonlinear distortion introduced by the PA is included in the reference signal [12].

The adaptive filter operates at the symbol rate to avoid the ill-condition problem of the autocorrelation matrix [18]. Thus, the PA output and the received signal are both down-shifted and lowpass filtered to baseband (as shown in Fig. 2) before being used as the regressor and the desired signal of the adaptive filter, respectively. It is found that the SI cancellation performance is sensitive to the sampling delay between the regressor and the received signal [19]. This problem can be solved by the digital SI cancellation scheme [19] shown in Fig. 1. The PA output is oversampled to twice the symbol rate, and the samples of the PA output are interleaved into two branches for SI cancellation. In such a case, the sampling delays between the PA output and the received signal on the two branches differ by half a symbol duration, which guarantees that reliable SI cancellation performance can be achieved in at least one of the branches [19].

A. ADAPTIVE NONLINEAR EQUALIZATION

It is assumed in the aforementioned digital cancellation scheme that the SI channel is linear. However, in practice, the pre-amplifier can also introduce the nonlinear distortion when the input signal level is high. As shown in Fig. 1, the received signal before and after the amplification is denoted as $x(t)$ and $\tilde{x}(t)$, respectively. The passband digitalized signal $\tilde{x}(n)$ is passed to the adaptive equalizer to equalize the nonlinear distortion introduced by the pre-amplifier. Afterwards, the equalized signal $\hat{x}(n)$ is used as the desired signal in the adaptive filter performing the SI channel estimation.

The Legendre polynomials are used as the BEM for the nonlinear equalization. We assume that the nonlinearity

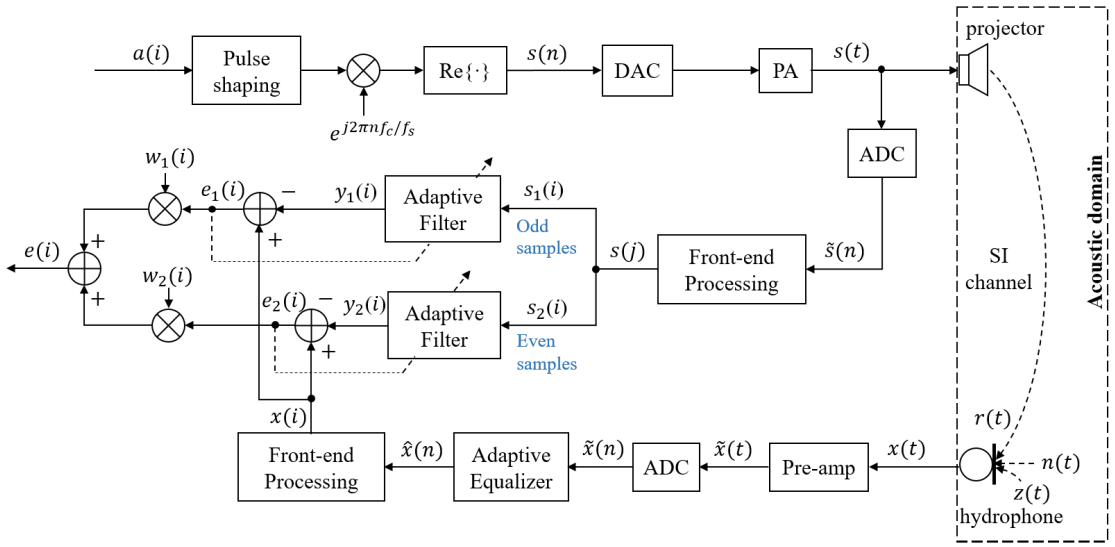

FIGURE 1. Block diagram of the FD UWA system. The analogue signals are denoted with a continuous time variable t, such as $s(t)$. The high sampling rate (passband) samples are denoted with index n; the symbol rate (baseband) samples are denoted with index i; $s(j)$ represents the PA output samples at twice the symbol rate; f_s and f_c represent the sampling frequency and carrier frequency, respectively; $w_1(i)$ and $w_2(i)$ are weight coefficients satisfying the condition $w_1(i) + w_2(i) = 1$ (see details in [19]); $e(i)$ is the residual signal of the SI canceller.

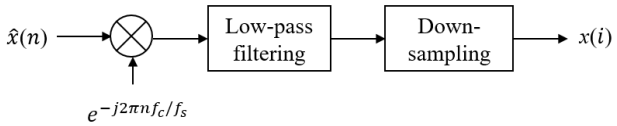

FIGURE 2. Front-end processing.

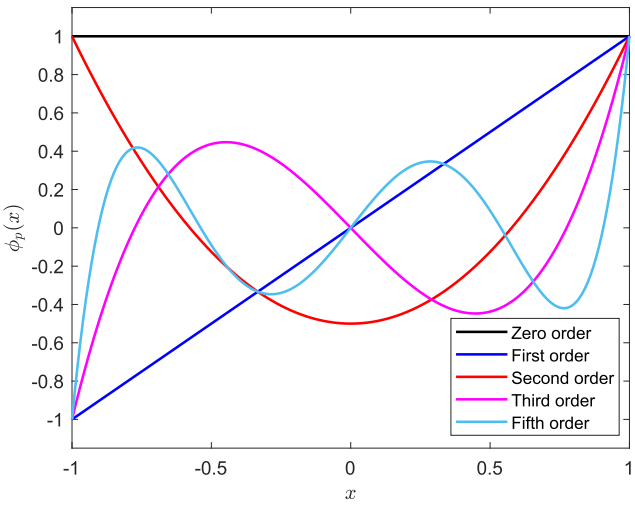

FIGURE 3. Legendre polynomials.

is memoryless. The output of the equalizer can be written as:

$$\hat{x}(n) = \tilde{x}(n) + \sum_{p \in P} c_p \phi_p(\tilde{x}(n)), \quad n = 1, \ldots, N, \tag{1}$$

where c_p are expansion coefficients, P is a set of Legendre polynomials and N is the number of samples used for equalization. The Legendre polynomials are defined on an interval $[-1, 1]$ as shown in Fig. 3. Before being applied to the equalizer, $\tilde{x}(n)$ is normalized to guarantee that the equalizer input is within this interval.

The general idea of the adaptive nonlinear equalizer is to find the expansion coefficients which minimize a cost function. The expansion coefficients are initialized to zero and the coordinate descent search is used to update the expansion coefficients. Let $\mathbf{u} = [-1, 1]$ be a direction vector with elements $u(d)$. At the mth iteration, for the dth direction, the pth expansion coefficient is updated as:

$$c_p^{(m)} = c_p^{(m-1)} + u(d) \cdot \delta, \tag{2}$$

where δ is a step size. The step size is initialized to $\delta = H$, where H is the maximum possible value of the expansion coefficients; see [20] for more details on the choice of H. For each tentative update of the expansion coefficient, the equalized signal vector $\hat{\mathbf{x}} = [\hat{x}(1), \ldots, \hat{x}(N)]^T$ and a cost function are computed. If the cost function is reduced, the expansion coefficient c_p is updated in the direction which minimizes the cost function. If $\mathbf{c} = [c_1, \ldots, c_{|P|}]$ remains the same after going through all the basis functions, the step size is reduced by a factor of two.

B. THE COST FUNCTIONS

Two cost functions are considered for the adaptive nonlinear equalization. The first one is based on the residual SI level after the SI cancellation. If the nonlinear distortion introduced by the pre-amplifier is equalized, the SI estimation performance will be improved, and thus a lower residual SI level can be achieved. The normalized MSE (NMSE) given in (9) is used to represent the residual SI level at the adaptive filter output. Thus, the NMSE is directly used as the cost function to evaluate the performance of the adaptive nonlinear equalizer. The algorithm of the equalizer with the MSE-based cost function is summarized in Algorithm 1.

Algorithm 1 Adaptive Nonlinear Equalizer (MSE-Based)

Input: $\tilde{\mathbf{x}}$
Output: $\hat{\mathbf{x}}$
Initialization: $\mathbf{c}(0) = \mathbf{0}$, $\delta = H$
Compute $\text{NMSE}_{\text{ref}} = \text{NMSE}$ as a reference
for each iteration m **do**
  Compute $\hat{\mathbf{x}}$ based on Equation (1)
  for the pth basis function **do**
    for the dth direction of search **do**
      Tentatively update $c_p^{(m)}$ based on Equation (2)
      Compute the equalizer output $\hat{\mathbf{x}}^{(m)}$
      Compute the NMSE
    end
    if the NMSE is reduced **then**
      Find the direction of update d minimizing the NMSE
      For the optimal direction, update $c_p^{(m)}$ based on Equation (2)
      Update NMSE_{ref}
    end
  end
  if c has not changed in this iteration **then**
    Reduce the step size δ: $\delta \leftarrow \delta/2$
  end
end

The main drawback of using the NMSE as the cost function is the high computational complexity. At each iteration, the SI canceller needs to be run $2|P|$ times, where $|P|$ (the cardinality of P) is the number of basis functions used for equalization. In some applications, the equalization based on minimizing the NMSE could be difficult to implement and therefore another cost function can be used for reduction in the complexity.

To reduce the complexity, we propose another cost function, which is derived in the frequency domain based on the signal power spectrum. For a linearly amplified signal, the spectrum is centred at the carrier frequency f_c. When there are nonlinear distortions introduced in the amplification, the signal spectrum also contains higher order harmonics centred at multiples of f_c. If the nonlinearity is compensated by the equalizer, the power of the harmonics will be reduced. Therefore, we define the cost function as the ratio of the powers of the harmonics over the fundamental signal power (harmonic-to-signal ratio, HSR), which is given by:

$$\text{HSR} = \frac{\text{P}_\text{H}}{\text{P}_\text{S}} = \frac{\sum_{q=2}^{Q} \sum_{k=f_3(q)/\Delta f}^{f_4(q)/\Delta f} \left|\hat{X}(k)\right|^2}{\sum_{k=f_1/\Delta f}^{f_2/\Delta f} \left|\hat{X}(k)\right|^2}, \tag{3}$$

and

$$f_1 = f_c - B/2, \quad f_3(q) = q(f_c - B/2),$$
$$f_2 = f_c + B/2, \quad f_4(q) = q(f_c + B/2),$$

where P_H is the power of the harmonics, P_S is the fundamental signal power, Q is the highest order of the harmonics considered, B represents the signal bandwidth, which is equal to the symbol rate, $\Delta f = f_s/N$ is the fast Fourier transform (FFT) frequency bin interval and and $\hat{X}(k)$ is computed as the FFT of the equalized signal $\hat{\mathbf{x}}$,

$$\hat{X}(k) = \sum_{n=0}^{N-1} \hat{x}(n) e^{-j2\pi kn/N}, \quad k = 1, \ldots, N. \tag{4}$$

It is found that, in some scenarios, using the HSR alone is not enough to guarantee good equalization performance. It occurs that the HSR can be reduced at the expense of higher sidelobes of the fundamental signal spectrum. It is shown in Section III-B that the sidelobe level of the equalized signal can increase significantly compared to the original level (see Fig. 10) when using the HSR as the cost function. To avoid such situations, additional constraints need to be applied to the sidelobes around the fundamental signal.

The power of the sidelobes (P_SL) can be computed as:

$$\text{P}_\text{SL} = \sum_{k \in B_\text{SL}/\Delta f} |\hat{X}(k)|^2, \tag{5}$$

where $B_\text{SL} = [f_c - b, f_c - a] \cup [f_c + a, f_c + b]$ defines the frequency range of the sidelobes, b can be chosen to be as large as $1.5B$ considering the wide spread of the sidelobes as shown in Fig. 10(f). The parameter a is chosen to be slightly larger than $B/2$ to avoid including frequencies with high power within the transition region, in that case, the value of P_SL cannot accurately reflect the level of the sidelobes.

The power of the sidelobes of the hydrophone output is computed at the start of the algorithm to be used as a reference P_ref. For each update of the expansion coefficients, we also compute P_SL of the equalized signal and compare it with P_ref. The pth expansion coefficient is updated if:

1) The updated sidelobe level is not increased ($\text{P}_\text{SL} \leq \text{P}_\text{ref}$).
2) The updated sidelobe level is not much lower than the original level ($\text{P}_\text{SL} > \eta \text{P}_\text{ref}$, where $\eta \in [0, 1]$ defines the threshold).

The second constraint is applied to avoid over-equalizing the hydrophone output. Since the PA output is used as the reference signal for SI cancellation, it is undesirable to equalize the nonlinear distortion introduced by the PA. The threshold parameter η depends on the level of nonlinear distortion introduced by the hydrophone pre-amplifier. The stronger the nonlinearity of the pre-amplifier, the smaller threshold parameter should be set.

To compute the cost function, the FFT of the equalized signal needs to be re-computed for each tentative update of

Algorithm 2 Adaptive Nonlinear Equalizer (HSR-Based)

Input: $\tilde{\mathbf{x}}$
Output: $\hat{\mathbf{x}}$
Initialization: $\mathbf{c}(0) = \mathbf{0}$, $\delta = H$, $\hat{\mathbf{x}} = \tilde{\mathbf{x}}$
for the pth basis function **do**
  Compute $X_\phi(p, k)$ based on Equation (7)
end
Compute $\hat{X}_{\text{past}}(k)$ based on Equation (4)
Compute $\text{HSR}_{\text{ref}} = \text{HSR}$ as a reference
Compute $\text{P}_{\text{ref}} = \text{P}_{\text{SL}}$ based on Equation (5)
for each iteration m **do**
  for the pth basis function **do**
    for the dth direction of search **do**
      Tentatively update $c_p^{(m)}$ based on Equation (2)
      Compute $\hat{X}_{\text{new}}(k)$ based on Equation (6)
      Compute HSR based on Equation (3)
    end
    if HSR is reduced **then**
      Find the direction of update d minimizing HSR
      Compute P_{SL} based on Equation (5)
      if $\eta\text{P}_{\text{ref}} < \text{P}_{\text{SL}} < \text{P}_{\text{ref}}$ **then**
        For the optimal direction, update $c_p^{(m)}$ based on Equation (2)
        Update the equalizer output $\hat{\mathbf{x}}$ and $\hat{X}_{\text{past}}(k)$
        Update HSR_{ref}
      end
    end
  end
  if $\mathbf{c}$ has not changed in this iteration **then**
    Reduce the step size δ: $\delta \leftarrow \delta/2$
  end
end

the expansion coefficients. To further reduce the complexity, $\hat{X}(k)$ is updated in a recursive way by:

$$\hat{X}_{\text{new}}(k) = \hat{X}_{\text{past}}(k) + \delta \cdot u(d) X_\phi(p, k), \tag{6}$$

and

$$X_\phi(p, k) = \sum_{n=0}^{N-1} \phi_p(x(n)) e^{-j2\pi kn/N}, \tag{7}$$

where $X_\phi(p, k)$ is the FFT of the pth basis function which only needs to be computed once for initialization. The algorithm with the HSR-based cost function is summarized in Algorithm 2.

III. EXPERIMENTAL RESULTS

In this section, we investigate the performance of the proposed adaptive nonlinear equalizer in two sets of water tank experiments.

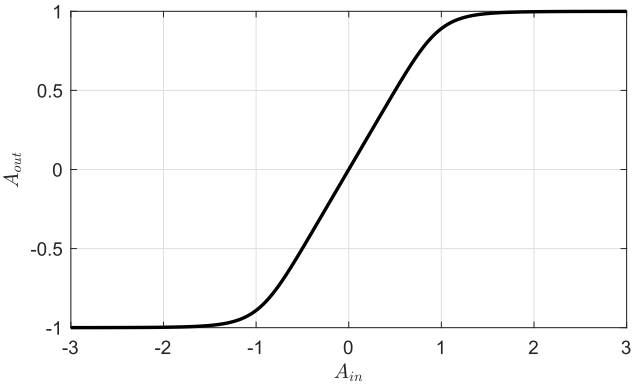

FIGURE 4. Rapp Model of the nonlinear amplitude response.

A. ARTIFICIALLY INTRODUCED NONLINEARITY

We first investigate the performance of the adaptive equalizer for artificially introduced nonlinear distortion in the received signal. The received signal $\tilde{x}(n)$ is recorded from a hydrophone without pre-amplifier [21] in a water tank experiment.

The experiment is conducted in a 1 m^3 plastic water tank. During the experiment, the projector is placed close to the surface and the hydrophone is placed close to the bottom. BPSK signals with the root-raised cosine pulse-shaping are transmitted. The parameters of the transmitted signal are set as follows: the roll-off factor is 0.2, the carrier frequency is $f_c = 12$ kHz, the bandwidth is $B = 1$ kHz. The sampling rate of the transmitted signal is $f_s = 96$ kHz and the baseband sampling rate is 1 kHz. Before the transmission, a 5 s silence period is recorded to measure the noise level at the receiver.

The Rapp Model [14] is used as the nonlinear model of the pre-amplifier. The amplitude distortion is given by:

$$\tilde{x}(t) = \frac{x(t)}{\left[|x(t)|^{2\alpha}\right]^{\frac{1}{2\alpha}}}, \tag{8}$$

where α is a parameter which controls the smoothness of the transition region of the response. In Fig. 4, we show the amplitude response generated by the Rapp model with $\alpha = 3$. The amplitude response can be divided into the linear zone, the transition zone and the saturation zone. We focus on the transition zone since the received signal cannot be equalized once it is saturated. The maximum absolute value of the input amplitude is set to 1, so that a substantial part of the signal will be in the transition zone.

The scheme shown in Fig. 1 is adopted for the digital SI cancellation. The sliding-window RLS (SRLS) adaptive filter [18] is used for the SI channel estimation as it is capable of providing good channel estimation performance [22]. The SI cancellation performance is evaluated by the NMSE:

$$\text{NMSE}(i) = \frac{|x(i) - \hat{\mathbf{h}}^H(i)\mathbf{s}(i)|^2}{P_x} \tag{9}$$

where $x(i)$ is the desired signal sample, $\hat{\mathbf{h}}(i)$ is an $L \times 1$ channel estimate, $\mathbf{s}(i) = [s(i), \ldots, s(i - L + 1)]^T$ is the regressor,

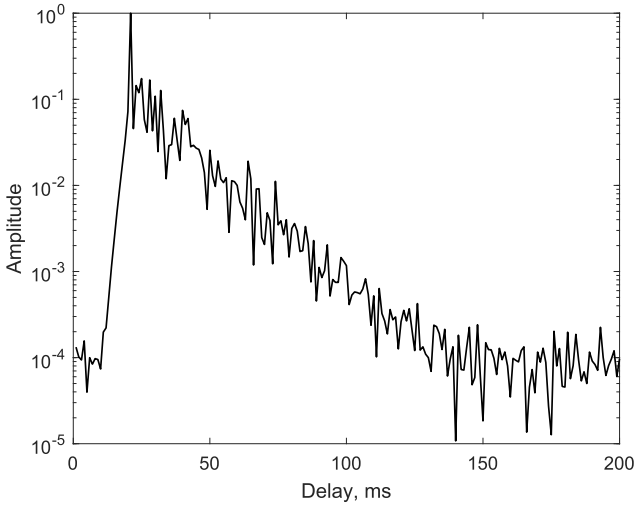

FIGURE 5. SI channel impulse response.

and $P_x = (\mathbf{x}^H\mathbf{x})/N$ is the average power of the desired signal. The averaged NMSE is computed by averaging the instantaneous NMSE(i) over an 8 s steady-state time interval.

The SI channel in the water tank has a long delay spread of around 150 ms as shown in Fig. 5. The NMSE performance of the digital canceller is shown in Fig. 7. The filter length is set to $L = 200$, and a sliding window length of $M = 4L = 800$ is used. The SI to noise ratio in this tank experiment is 55 dB. A steady-state NMSE of -53 dB is achieved when we use the original hydrophone output as the desired signal. This NMSE level is used as a benchmark for evaluating the performance of the adaptive equalizer. The steady-state NMSE degrades to -46 dB when the hydrophone output affected by the artificial nonlinearity shown in Fig. 4 is used as the desired signal.

We first adapt the equalizer using the MSE-based cost function. The initial step size is set to $H = 0.1$. To equalize the nonlinearity which has the amplitude response shown in Fig. 4, the Legendre polynomials of odd orders, specifically the third, fifth and seventh-order Legendre polynomials are used. As the MSE-based approach requires the adaptive filtering in each iteration, a small number of iterations $N_u = 10$ is used to reduce the complexity. Using this approach, the average NMSE is reduced to about -53 dB.

Then, we investigate the performance of the adaptive equalizer which updates the expansion coefficients using the HSR criterion. The signal power spectra before and after introducing the artificial nonlinearity are shown in Fig. 6 (a) and (b), respectively. The zoomed spectra around the third harmonic are shown in (d) and (e). It can be seen that the spread of the third harmonic of the original hydrophone output is wider after introducing the nonlinear distortion. Based on our computation, the HSR is increased by 4.1 dB after adding the nonlinear distortion. For equalization, we use the same initial step size as in the MSE-based approach. The number of iterations is $N_u = 100$. The power of the sidelobes

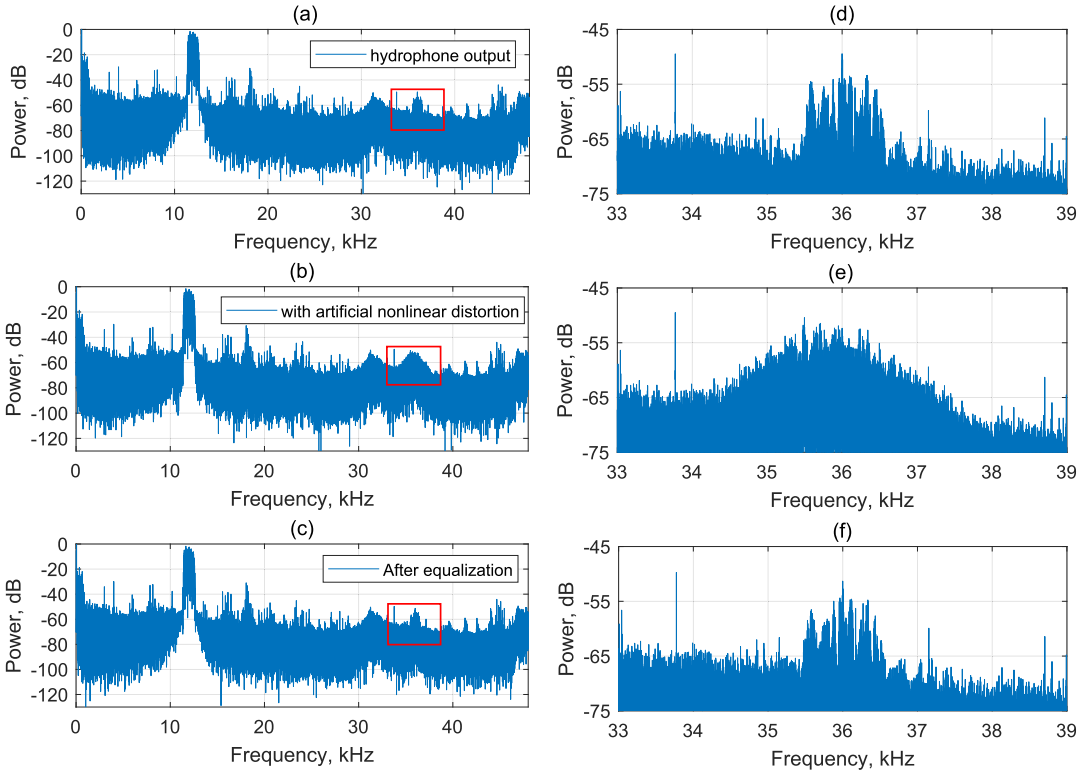

FIGURE 6. Power spectra of the signals: (a) original hydrophone output; (b) hydrophone output with the artificial nonlinear distortion; (c) nonlinear equalizer output. Zoomed plots of the spectra in (a), (b), (c) are shown in (d), (e), (f), respectively.

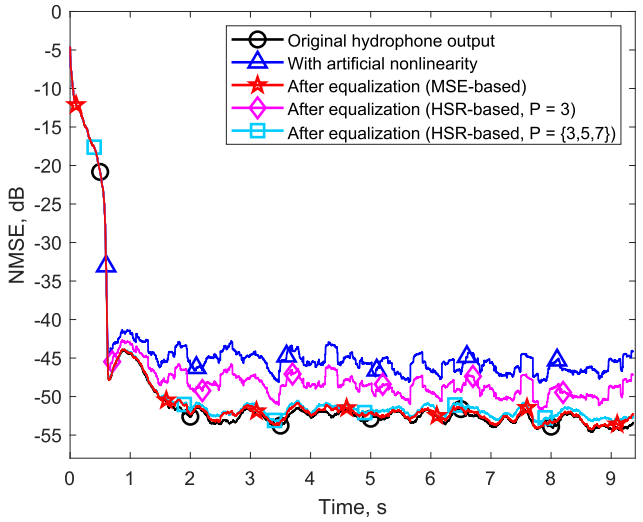

FIGURE 7. Comparison of the NMSE performance with the simulation data. The NMSE curves are smoothed by a 200 ms rectangular window.

is computed in the interval $[f_c - 1.5B, f_c - 0.7B] \cup [f_c + 0.7B, f_c + 1.5B]$. We use $\eta = 0.7$ in the threshold of the second constraint.

The majority of the complexity of the nonlinear equalizer comes from the computation of the cost function, which needs to be done $2|P|N_u$ times. The complexity of computing the NMSE using the SRLS adaptive filter is about $16NL^2B/f_s$ real-valued arithmetic operations. For the HSR-based cost function, FFT of the equalizer input and FFT of basis functions need to be computed once for initialization, which requires about $(|P| + 1)N\log(N)$ operations. Then in N_u iterations, the spectrum of the equalized signal is computed recursively as shown in (6) at N_f frequencies used in (3) and (5); in our case, $N_f \approx 8NB/f_s$. For a 9.5 s interval, the total number of passband samples is $N = 9.12 \times 10^5$. For $N_u = 10$, the complexity of the NMSE-based equalizer is 3.7×10^{11} arithmetic operations. For the HSR-based equalizer, the initialization requires about 0.5×10^8 operations; for $N_u = 100$ recursions in (6), about 0.9×10^8 operations are required; computation in (3) and (5) require further 0.9×10^8 operations. Hence, the total complexity of the HSR-based equalizer is about 2.3×10^8 operations, which is about 1600 times lower than that of the NMSE-based equalizer.

As shown in Fig. 7, the steady-state NMSE is reduced from -46 dB to about -48 dB when only the third-order Legendre polynomial is used for equalization. The higher the order of the polynomials included in the model, the better the achievable performance. The NMSE is further reduced to -52dB when we include the third, fifth and seventh-order Legendre polynomials. The zoomed power spectrum of the signal after equalization shown in Fig. 6 (f) also demonstrates the effectiveness of the nonlinear equalizer as the spectral shape of the third harmonic almost returns to the same shape as that of the original hydrophone output shown in Fig. 6 (d). It is seen that both approaches work well in equalizing the artificial nonlinearity added to the received signal.

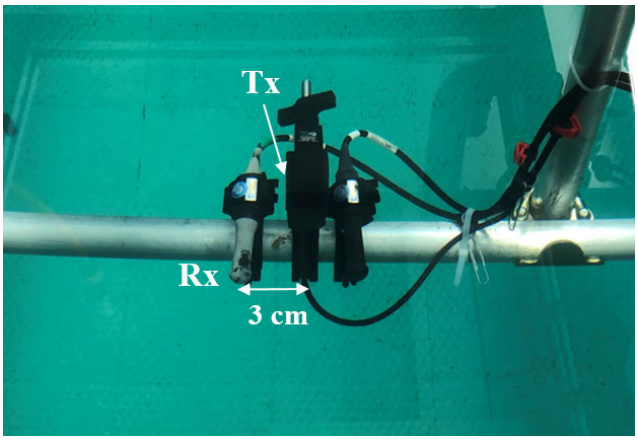

FIGURE 8. Experimental setup in an anechoic water tank.

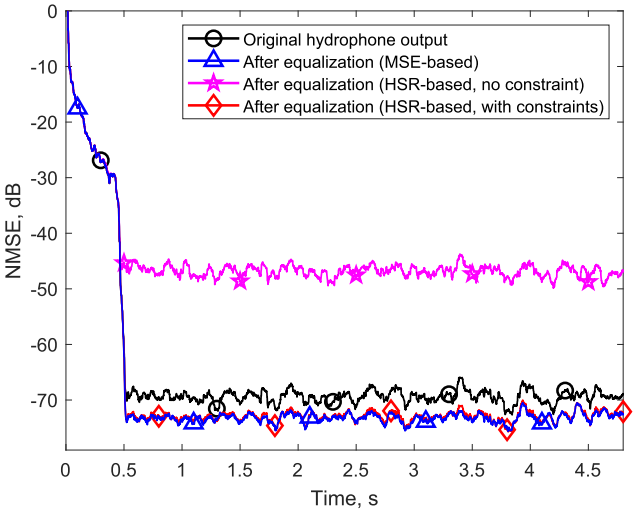

FIGURE 9. Comparison of the NMSE performance in the anechoic water tank. The NMSE curves are smoothed by a rectangular window of length 50 ms.

B. USING HYDROPHONE WITH PRE-AMPLIFIER

We then evaluate the performance of the proposed nonlinear equalizer with the experimental data recorded from the hydrophone with pre-amplifier [23] in an anechoic water tank. The distance between the projector (Tx) and hydrophone (Rx) is 3 cm as shown in Fig. 8. We transmit BPSK signals at $f_c = 14$ kHz carrier frequency with $B = 1$ kHz bandwidth. The sampling frequency is $f_s = 96$ kHz. The SI to noise ratio is around 85 dB.

Unlike the channel impulse response shown in Fig. 5, the SI channel in the anechoic water tank only contains the direct path and the first surface reflection. The other reflections are absorbed by the tank walls. The SRLS adaptive filter is used for the SI channel estimation. We use the filter length $L = 50$ and a sliding window length of $M = 500$. When the original hydrophone output is used for SI cancellation, an average NMSE level of -69 dB is achieved.

Then we apply the MSE-based adaptive equalizer with the third Legendre polynomials. For this data record,

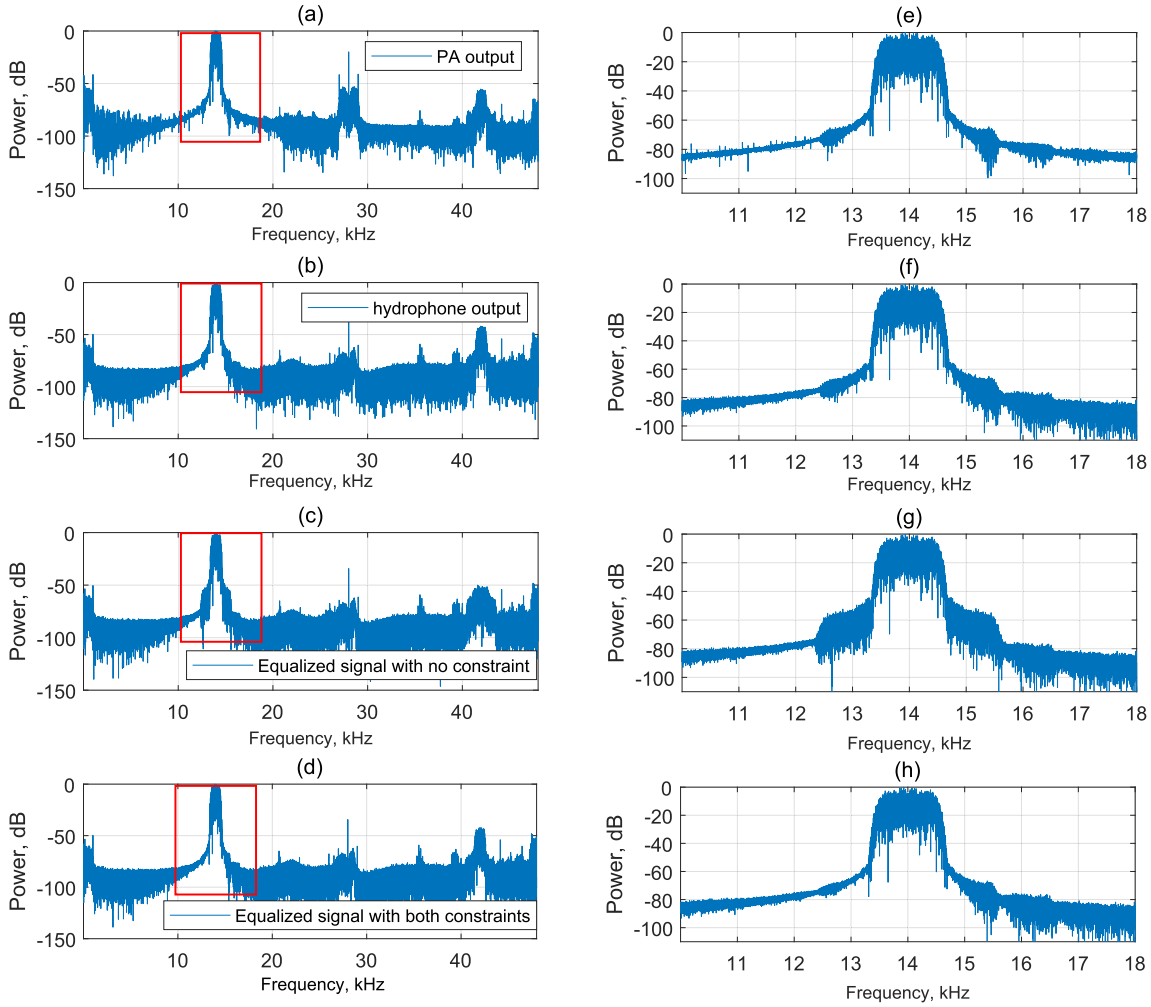

FIGURE 10. Power spectra of the signals: (a) PA output;(b) Original hydrophone output; (c) Signal equalized using HSR as the cost function; (d) Signal equalized using HSR with both constraints. Zoomed plots of the spectra in (a), (b), (c) and (d) are shown in (e), (f), (g) and (h), respectively.

the improvement achieved by including higher order polynomials is minor, thus we only use one basis function to reduce the complexity. The initial step size is $H = 0.01$, and the number of updates is $N_u = 10$. It can be seen in Fig. 9 that the average NMSE is reduced to -73 dB. An improvement of about 4 dB in the NMSE performance is achieved.

For the HSR-based equalizer, we also use the third-order Legendre polynomial as the basis function and with the same step size. The number of updates is $N_u = 20$. In Fig. 10, we show the power spectra of the PA output, the hydrophone output and the equalized signals under different conditions. Zoomed plots of the spectra are also shown to provide a clear visualisation for the comparison. It can be seen in Fig. 10 (g) that the sidelobes of the signal are significantly increased when the HSR with no constraint is used, which results in a poor NMSE performance as shown in Fig. 9.

The NMSE performance is around -68 dB without the second constraint. This is due to the over-equalization of the nonlinearity in the hydrophone output. There should be a threshold which defines the maximum reduction in the sidelobe level. In this scenario, we use $\eta = 0.97$. In practice, the threshold can be tuned based on the signal spectrum and the MSE performance as the complexity of the equalizer is significantly lower when using the HSR-based cost function, since there is no need for the adaptive filtering providing the highest contribution into the algorithm complexity. After applying both constraints to the cost function, an NMSE of -73 dB is achieved, which is the same as the NMSE performance of the MSE-based equalization.

IV. CONCLUSIONS

In this paper, we have proposed a technique for equalizing the nonlinear distortion of signals introduced by the hydrophone pre-amplifier in FD UWA systems. The Legendre polynomials are used as basis functions for the adaptive nonlinear equalization. The expansion coefficients of the basis functions are updated recursively to reduce the cost function. We have considered two cost functions, one is the NMSE and the other is derived based on the

signal power spectrum. At each iteration, the coefficients are updated using the dichotomous coordinate descent search.

The performance of the nonlinear equalizer is evaluated in two water tank experiments. In the first experiment, artificial nonlinear distortion described by the Rapp model is introduced to the received signal from the hydrophone without pre-amplifier. It is shown that the proposed technique provides close to perfect equalization of the introduced nonlinearity. For the second experiment, we use the experimental data obtained from a hydrophone with pre-amplifier. An improvement in the SI cancellation performance of 4 dB has been achieved when applying the nonlinear equalizer.

ACKNOWLEDGMENT

The authors would like to thank the colleague from the University of York, N. Morozs for providing help in setting up the experiments and the colleagues from the Newcastle University, C. Tsimendis, J. Neasham, and C. Healy for providing the experimental site and technical support during the experiments.

REFERENCES

[1] J. I. Choi, M. Jain, K. Srinivasan, P. Levis, and S. Katti, "Achieving single channel, full duplex wireless communication," in *Proc. 16th Annu. Int. Conf. Mobile Comput. Netw. (MobiCom)*, 2010, pp. 1–12.

[2] M. Duarte and A. Sabharwal, "Full-duplex wireless communications using off-the-shelf radios: Feasibility and first results," in *Proc. Conf. Rec. Forty 4th Asilomar Conf. Signals, Syst. Comput.*, Nov. 2010, pp. 1558–1562.

[3] M. Jain, J. I. Choi, T. Kim, D. Bharadia, S. Seth, K. Srinivasan, P. Levis, S. Katti, and P. Sinha, "Practical, real-time, full duplex wireless," in *Proc. 17th Annu. Int. Conf. Mobile Comput. Netw. (MobiCom)*, 2011, pp. 301–312.

[4] D. Korpi, T. Riihonen, V. Syrjälä, L. Anttila, M. Valkama, and R. Wichman, "Full-duplex transceiver system calculations: Analysis of ADC and linearity challenges," *IEEE Trans. Wireless Commun.*, vol. 13, no. 7, pp. 3821–3836, Jul. 2014.

[5] G. Qiao, S. Gan, S. Liu, and Q. Song, "Self-interference channel estimation algorithm based on maximum-likelihood estimator in in-band full-duplex underwater acoustic communication system," *IEEE Access*, vol. 6, pp. 62324–62334, 2018.

[6] *Hydrophone Handbook*. Accessed: Feb. 6, 2020. [Online]. Available: http://www.ondacorp.com

[7] L. Anttila, D. Korpi, V. Syrjala, and M. Valkama, "Cancellation of power amplifier induced nonlinear self-interference in full-duplex transceivers," in *Proc. Asilomar Conf. Signals, Syst. Comput.*, Nov. 2013, pp. 1193–1198.

[8] J. Butler and C. Sherman, *Transducers and Arrays for Underwater Sound*. Cham, Switzerland: Springer, 2016.

[9] Y. Liu, X. Quan, W. Pan, S. Shao, and Y. Tang, "Nonlinear distortion suppression for active analog self-interference cancellers in full duplex wireless communication," in *Proc. IEEE Globecom Workshops (GC Wkshps)*, Dec. 2014, pp. 948–953.

[10] M. S. Sim, M. Chung, D. Kim, J. Chung, D. K. Kim, and C.-B. Chae, "Nonlinear self-interference cancellation for full-duplex radios: From link-level and system-level performance perspectives," *IEEE Commun. Mag.*, vol. 55, no. 9, pp. 158–167, Jun. 2017.

[11] F. H. Gregorio, G. J. Gonzalez, J. Cousseau, T. Riihonen, and R. Wichman, "Predistortion for power amplifier linearization in full-duplex transceivers without extra RF chain," in *Proc. IEEE Int. Conf. Acoust., Speech Signal Process. (ICASSP)*, Mar. 2017, pp. 6563–6567.

[12] L. Shen, B. Henson, Y. Zakharov, and P. Mitchell, "Digital self-interference cancellation for full-duplex underwater acoustic systems," *IEEE Trans. Circuits Syst. II, Exp. Briefs*, vol. 67, no. 1, pp. 192–196, Jan. 2020.

[13] I. Gradshteyn and I. Ryzhik, *Table of Integrals, Series and Products*. Amsterdam, The Netherlands: Elsevier, 2014.

[14] C. Rapp, "Effects of HPA-nonlinearity on a 4-DPSK/OFDM-signal for a digital sound broadcasting signal," in *Proc. 2nd Eur. Conf. Satell. Commun.*, 1991, pp. 179–184.

[15] D. Korpi, Y.-S. Choi, T. Huusari, L. Anttila, S. Talwar, and M. Valkama, "Adaptive nonlinear digital self-interference cancellation for mobile inband full-duplex radio: Algorithms and RF measurements," in *Proc. IEEE Global Commun. Conf. (GLOBECOM)*, Dec. 2015, pp. 1–7.

[16] D. Korpi, J. Tamminen, M. Turunen, T. Huusari, Y.-S. Choi, L. Anttila, S. Talwar, and M. Valkama, "Full-duplex mobile device: Pushing the limits," *IEEE Commun. Mag.*, vol. 54, no. 9, pp. 80–87, Sep. 2016.

[17] G. Qiao, S. Gan, S. Liu, L. Ma, and Z. Sun, "Digital self-interference cancellation for asynchronous in-band full-duplex underwater acoustic communication," *Sensors*, vol. 18, no. 6, pp. 1700–1716, 2018.

[18] S. Haykin, *Adaptive Filter Theory*. Upper Saddle River, NJ, USA: Prentice-Hall, 2002.

[19] L. Shen, B. Henson, Y. Zakharov, and P. Mitchell, "Robust digital self-interference cancellation for full-duplex UWA systems: Lake experiments," in *Proc. Underwater Acoust. Conf. Exhib.*, 2019, pp. 243–250.

[20] Y. V. Zakharov, G. P. White, and J. Liu, "Low-complexity RLS algorithms using dichotomous coordinate descent iterations," *IEEE Trans. Signal Process.*, vol. 56, no. 7, pp. 3150–3161, Jul. 2008.

[21] *Low Noise Broadband Hydrophone Without Preamplifier*. Accessed: Feb. 26, 2020. [Online]. Available: https://www.benthowave.com/products/BII-7010Hydrophone.html

[22] Y. V. Zakharov and J. Li, "Sliding-window homotopy adaptive filter for estimation of sparse UWA channels," in *Proc. IEEE Sensor Array Multichannel Signal Process. Workshop (SAM)*, Jul. 2016, pp. 1–4.

[23] *Neptune Sonar-Hydrophones With Pre-Amplifiers. Accessed:* Feb. 26, 2020. [Online]. Available: http://www.neptune-sonar.co.uk/product-category/standard-transducer-products/hydrophones/hydrophone-with-pre-amplifier/

LU SHEN (Graduate Student Member, IEEE) received the M.Sc. degree (Hons.) in digital signal processing from the University of York, York, U.K., in 2016, where she is currently pursuing the Ph.D. degree in electronic engineering with the Communication Technologies Research Group, Department of Electronic Engineering. Her research interests include adaptive signal processing and underwater acoustic communications.

BENJAMIN HENSON (Member, IEEE) received the M.Eng. degree in electronic engineering and the M.Sc. degree in natural computation from the University of York, York, U.K., in 2001 and 2011, respectively, and the Ph.D. degree in electronic engineering from the Communication Technologies Research Group, University of York, in 2018.

From 2002 to 2008, he was an Engineer with Snell and Wilcox Ltd., designing broadcast equipment. From 2008 to 2009, he worked with SRD Ltd., on imaging sonar designs. From 2011 to 2013, he worked on laser measurement equipment with Renishaw plc. He is currently a Research Associate with the Communication Technologies Research Group, Department of Electronic Engineering, University of York. His research interests include signal and image processing and acoustics.

YURIY ZAKHAROV (Senior Member, IEEE) received the M.Sc. and Ph.D. degrees in electrical engineering from the Power Engineering Institute, Moscow, Russia, in 1977 and 1983, respectively.

From 1977 to 1983, he was with the Special Design Agency, Moscow Power Engineering Institute. From 1983 to 1999, he was with the N. N. Andreev Acoustics Institute, Moscow. From 1994 to 1999, he was a DSP Group Leader with Nortel. Since 1999, he has been with the Communication Technologies Research Group, Department of Electronic Engineering, University of York, U.K., where he is currently a Reader. His research interests include signal processing, communications, and underwater acoustics.

PAUL D. MITCHELL (Senior Member, IEEE) has previously worked with BT and QinetiQ. He is currently a Reader in electronic engineering with the University of York, U.K. He has secured more than £2.3M and €4.7M funding as a Principal and a Co-Investigator. His current projects include Research Council grants on smart dust for large scale underwater wireless sensing, full-duplex underwater acoustic communications, as well as industrial projects. He is the author of over 130 refereed journal articles and conference papers. He has served on numerous international conference programme committees, including ICC and VTC. His primary research interests include resource management, medium access control for underwater acoustic communication networks, terrestrial wireless sensor networks, and satellite systems.

Mr. Mitchell is a member of the IET. He was the General Chair of the International Symposium on Wireless Communications Systems, in 2010. He currently serves as an Associate Editor for *IET Wireless Sensor Systems* journal, the *International Journal of Distributed Sensor Networks*, and *MDPI Electronics*. He has experience as a Guest Editor and as a Reviewer for a number of the IEEE, ACM, and IET journals.